Vibrational Predissociation Rates and Final State Distributions for He−ICl and He−I_2 Using a Computationally Simple Method

Jeonghee Seong and Hosung Sun

Department of Chemistry, Sungkyunkwan University, Suwon 440-746, and Center for Molecular Science, KAIST, Taejon, 305-701, Korea

Mark A. Ratner and George C. Schatz*

Department of Chemistry, Northwestern University, Evanston, Illinois 60208-3113

R. B. Gerber

Fritz Haber Institute for Molecular Dynamics, Hebrew University, Jerusalem, Israel, and Department of Chemistry, University of California at Irvine, Irvine, California, 92697

Received: February 19, 1998; In Final Form: April 28, 1998

The vibrational predissociation rates of triatomic van der Waals complexes were investigated by a new, computationally simple method. The method is based on three approximations: (a) metastable vibrationally excited states of the complex are described by the vibrational self-consistent field (VSCF) approximation, (b) the coupling among the rotational states of the dissociating diatomic fragment is treated by the infinite order sudden (IOS) approximation, and (c) the vibrational transition that leads to dissociation is treated by the distorted wave Born approximation (DWBA). The predissociation rates, the product rotational state distributions, and the lifetimes of vibrationally excited states of He−ICl and He−I_2 are all computed and are in reasonable agreement with other theoretical and/or experimental results. The suggested VSCF−DWBA−IOS scheme is found to be a very simple but efficient theoretical tool to investigate the dissociation dynamics of van der Waals complexes.

I. Introduction

Van der Waals complexes, e.g., molecules weakly bound to rare gas atoms, have attracted considerable attention, both experimentally and theoretically.[1−21] Techniques such as high-resolution IR absorption spectroscopy, Fourier-transform infrared spectroscopy, and microwave spectroscopy provide a wealth of information on the structure and the vibrational energy levels of van der Waals complexes. In many weakly bound molecules the deviation from harmonic behavior is very large, even in the vibrational ground state. It remains a challenge to obtain accurate energy level structure for these molecules from the potential energy functions and to interpret the level structure in terms of the vibrational dynamics involved.

Many theoretical approaches have been applied to study the vibrational states of van der Waals complexes. Our aim here is to test an approximate scheme that scales only linearly with molecular size, so that it can be applied efficiently to large systems. The vibrational self-consistent field model (VSCF) has this convenient scaling property. The VSCF and related configuration interaction (CI) methods are widely used in electronic structure calculations, but vibrational structure calculations using VSCF and CI are not frequently reported. In the VSCF method,[8,12,22−27] each vibrational mode is described as moving in an effective field that is the average of the full potential over the motions of all the other modes. Each vibrational mode is described by wave functions called modal wave functions corresponding to orbitals in electronic structure theory. In the VSCF method, correlation between modes is not included. Therefore, the validity and accuracy of the approximation depend on the choice of coordinates used in the calculations because each modal wave function is dictated by the coordinates chosen. The correlation part missing in the VSCF approximation is incorporated in the CI method. In CI the true vibrational wave functions are expressed as a linear combination of configurations, each of which is a product of modal wave functions. The CI matrix is diagonalized to obtain vibrational energies and wave functions; these become exact (on the assumed potential energy surface) for a complete expansion.

Extensive theoretical and experimental efforts have been made to understand the dynamics of triatomic systems, including vibrational predissociation. Triatomic van der Waals complexes provide ideal model systems for predissociation studies because the electronic states involved are well-studied, the potential energy surfaces are well-characterized, and the relevant quantities (such as transition dipole moments) are known. In the present work we develop a new but simple method to investigate the vibrational predissociation process. We treat the initial (metastable) state of the complex in the VSCF approximation; the predissociation dynamics is simplified by applying the infinite order sudden (IOS) approximation to the coupling among the rotational states of the molecular fragment in the course of the dissociation, and finally the distorted wave Born approximation (DWBA) is used to express the decay rate of the initial state into products. Both the sudden and distorted wave approximations are well-known from scattering theory,[28] and as we shall see, physical considerations justify the present

10.1021/jp9812132 CCC: $15.00
Published on Web 06/06/1998

application to vibrational predissociation for the systems and conditions that are commonly of interest.

This new scheme is extremely simple, so we have performed some test calculations for He−ICl and He−I_2 to assess its accuracy. In these calculations, the VSCF approximation is tested by comparison with vibrational energy levels calculated using other methods, and then the IOS and DWBA approximations are tested by calculating dissociation rates and comparing with accurate values from other theory and/or experiment.

The present VSCF−IOS−DWBA method has some similarity to a method that was used previously in studies of atom−molecule inelastic collisions.[29,30] In this study, the IOS method was used to describe rotational coupling and DWBA was used to determine scattering cross sections. Another related study done previously by some of us[20] was concerned with collinear models of triatomic predissociation dynamics. Here the VSCF method was used to describe the initial states and DWBA for the predissociation rate.

In section II a brief summary of our proposed method, i.e., VSCF−DWBA−IOS, is provided. Section III explains the potential energy functions and numerical aspects of computations. The calculational results and discussion are provided in section IV, and some conclusions are given in section V.

II. Method

The present study extends our earlier method for studying triatomic systems.[20] Jacobi coordinates are chosen to describe the triatomic system, AB−C, where C is a rare gas atom and AB is a covalently bonded diatom. The Hamiltonian H for the AB−C system is written as, in atomic units,

$$H(r, R, \theta) = \frac{-1}{2\mu_1 r^2}\frac{\partial}{\partial r} r^2 \frac{\partial}{\partial r} - \frac{1}{2\mu_2 R^2}\frac{\partial}{\partial R}\left(R^2 \frac{\partial}{\partial R}\right) + \frac{\mathbf{j}^2}{2\mu_1 r^2} + \frac{\mathbf{l}^2}{2\mu_2 R^2} + V(r, R, \theta) \quad (1)$$

where r is the internuclear distance between atoms A and B, R is the distance between the center of mass of the diatom AB and atom C, and θ is the angle between two vectors associated with r and R. μ_1 is the reduced mass of atoms A and B, and μ_2 is the reduced mass of diatom AB and atom C, i.e., $\mu_1 = m_A m_B/(m_A + m_B)$ and $\mu_2 = m_C(m_A + m_B)/(m_A + m_B + m_C)$. $\mathbf{j}$ and $\mathbf{l}$ are two angular momenta associated with r and R, respectively. For $\mathbf{J} = \mathbf{j} + \mathbf{l} = 0$, we have

$$\mathbf{j}^2 = \mathbf{l}^2 = \frac{-1}{\sin\theta}\frac{\partial}{\partial\theta}\left(\sin\theta \frac{\partial}{\partial\theta}\right) \quad (2)$$

$V(r, R, \theta)$ is the potential energy function. The range of θ is defined from 0 to π, and the range of r and R is from 0 to ∞. The Schrödinger equation is

$$H(r, R, \theta)\,\Phi(r, R, \theta) = E\Phi(\mathrm{r}, \mathrm{R}, \theta) \quad (3)$$

where E is the vibrational energy and $\Phi(r, R, \theta)$ is the vibrational wave function. If we replace $\Phi(r, R, \theta)$ with $\Psi(r, R, \theta)/rR$, the reduced equation is

$$H(r, R, \theta)\,\Psi(r, R, \theta) = E\Psi(r, R, \theta) \quad (4)$$

where $\Psi(r, R, \theta)$ is normalized such that $\int\int\int|\Psi(r, R, \theta)|^2 \sin\theta\, \mathrm{d}\theta\, \mathrm{d}R\, \mathrm{d}r = 1$. The reduced Hamiltonian is

$$H(r, R, \theta) = \frac{-1}{2\mu_1}\frac{\partial^2}{\partial r^2} - \frac{1}{2\mu_2}\frac{\partial^2}{\partial R^2} + \frac{\mathbf{j}^2}{2\mu_1 r^2} + \frac{\mathbf{l}^2}{2\mu_2 R^2} + V_1(r) + V_2(r, R, \theta) \quad (5)$$

Here $V_1(r)$ is the potential energy function for diatom AB and $V_2(r, R, \theta)$ is the remaining potential, i.e., $V(r, R, \theta) = V_1(r) + V_2(r, R, \theta)$.

Equation 1 is solved for bound states using VSCF and for dissociation using IOS. If the bound state solution is designated as $\Psi^{\mathrm{i}}_{\nu_1\nu_2\nu_3}(r, R, \theta)$ and the dissociating state solution as $\Psi^{\mathrm{f}}_{\nu'_1\mathrm{j}}(r, R, \theta)$, DWBA yields the dissociation rate R as

$$R(\nu_1\nu_2\nu_3 \rightarrow \nu'_1\mathrm{j}) = \frac{2\pi}{\hbar}\rho(E)|\langle\Psi^{\mathrm{f}}_{\nu'_1\mathrm{j}}(r, R, \theta)|V_{\mathrm{c}}|\Psi^{\mathrm{i}}_{\nu_1\nu_2\nu_3}(r, R, \theta)\rangle|^2 \quad (6)$$

ν_i (i = 1, 2, 3) are the vibrational quantum numbers of the triatom AB−C, ν_1' is the quantum number associated with AB molecular vibration, and j is the quantum number associated with AB molecular rotation. The correlation potential V_c and the density of states ρ(E) will be defined later.

A. VSCF Approximation. In VSCF each vibrational mode is described as moving in an effective field, being the average of the full potential over the motions of all the other modes. Each vibrational mode consists of wave functions called modal wave functions corresponding to orbitals in electronic structure theory. Since each modal is associated with a formally separate Hamiltonian, the VSCF method clearly involves an assumption of mutual separability of vibrational modes. However, the VSCF modes are different from normal modes. While normal modes are assumed to be independent of each other, in VSCF the effect of other modes is incorporated in an average sense.

The outline of the VSCF procedure is as follows. We assume that the bound state wave function can be approximated as[20,22]

$$\Psi^{\mathrm{i}}_{\nu_1\nu_2\nu_3}(r, R, \theta) \approx \Psi^{\mathrm{SCF}}_{\nu_1\nu_2\nu_3}(r, R, \theta) = \varphi^1_{\nu_1}(\mathrm{r})\,\varphi^2_{\nu_2}(\mathrm{R})\,\varphi^3_{\nu_3}(\theta) \quad (7)$$

and

$$H^{\mathrm{SCF}}(r, R, \theta)\,\Psi^{\mathrm{SCF}}_{\nu_1\nu_2\nu_3}(r, R, \theta) = E^{\mathrm{SCF}}_{\nu_1\nu_2\nu_3}\Psi^{\mathrm{SCF}}_{\nu_1\nu_2\nu_3}(r, R, \theta) \quad (8)$$

The quantum number ν_1 corresponds to the vibrational motion of the diatom AB, ν_2 is the quantum number for the van der Waals bond stretching motion, and ν_3 is the corresponding bending motion. Then the Hamiltonian is partitioned as and

$$\mathrm{H}^{\mathrm{SCF}}(r, R, \theta) = h^1(r) + h^2(R) + h^3(\theta) \quad (9)$$

the modal wave functions φ satisfy

$$h^1(r)\,\varphi^1_{\nu_1}(r) = \epsilon^1_{\nu_1}\varphi^1_{\nu_1}(r) \quad (10a)$$

$$\mathrm{h}^2(R)\,\varphi^2_{\nu_2}(R) = \epsilon^2_{\nu_2}\varphi^2_{\nu_2}(R) \quad (10b)$$

$$\mathrm{h}^3(\theta)\,\varphi^3_{\nu_3}(\theta) = \epsilon^3_{\nu_3}\varphi^3_{\nu_3}(\theta) \quad (10c)$$

where ϵ_{ν_1}, ϵ_{ν_2}, and ϵ_{ν_3} are modal eigenvalues, ν_1, ν_2, and ν_3 are vibrational quantum numbers associated with coordinates r, R, and θ, respectively, and

$$h^1(r) = -\frac{1}{2\mu_1}\frac{\partial^2}{\partial r^2} + \frac{1}{2\mu_1 r^2}\langle\mathbf{j}^2\rangle_\theta + V_1(r) + \langle V_2(r, R, \theta)\rangle_{R,\theta} \quad (11a)$$

$$h^2(R) = -\frac{1}{2\mu_2}\frac{\partial^2}{\partial R^2} + \frac{1}{2\mu_2 R^2}\langle \mathbf{l}^2\rangle_\theta + \langle V_2(r, R, \theta)\rangle_{r,\theta} \quad (11b)$$

$$h^3(\theta) = \left\langle \frac{1}{2\mu_1 r^2}\right\rangle_r \mathbf{j}^2 + \left\langle \frac{1}{2\mu_2 R^2}\right\rangle_R \mathbf{l}^2 + \langle V_2(r, R, \theta)\rangle_{r,R} \quad (11c)$$

The subscripts after each set of brackets $\langle\rangle$ indicate that the quantity is an integral in the subscripted variable over the modal functions. The total VSCF energy for the (ν_1, ν_2, ν_3) state is

$$E^{\mathrm{i}}_{\nu_1\nu_2\nu_3} \approx E^{\mathrm{SCF}}_{\nu_1\nu_2\nu_3} + E_{\mathrm{cor}} = \epsilon^1_{\nu_1} + \epsilon^2_{\nu_2} + \epsilon^3_{\nu_3} + E_{\mathrm{cor}} \quad (12a)$$

where the correction energy E_{cor} is

$$E_{\mathrm{cor}} = -\left\langle \frac{1}{2\mu_1 r^2}\right\rangle_r \langle \mathbf{j}^2\rangle_\theta - \left\langle \frac{1}{2\mu_2 R^2}\right\rangle_R \langle \mathbf{l}^2\rangle_\theta - 2\langle V_2(r, R, \theta)\rangle_{r,R,\theta} \quad (12b)$$

The VSCF equations are iteratively solved to obtain converged modal eigenfunctions and eigenenergies for a prechosen reference (ν_1, ν_2, ν_3) bound state.

Instead of basis function representations, we used numerical grid representations for modal functions. As we see in eqs 11a and 11b, the differential equations involving the r and R coordinates can be easily solved. However, the θ coordinate in eq 11c imposes a small problem in numerical representation. To obtain numerical representations for $\varphi^3_{\nu_3}(\theta)$, we adopt the discrete variable representation (DVR) proposed by Light and Bacic.[21,31,32] The DVR is introduced in order to simplify the approximate evaluation and manipulation of the Hamiltonian operator. In particular, the kinetic energy operator, easily evaluated in the variational basis representation, is transformed to the DVR, whereas the remaining potential operators, which are difficult to evaluate in the basis representation, are approximated directly in DVR. In DVR a unitary transformation matrix $\mathbf{T}$ is defined as $\mathbf{T}_{\mathbf{l}\chi_\alpha} = ((2\mathbf{l}+1)/2)^{1/2}\omega^{1/2}_{\chi_\alpha} P_{\mathbf{l}}(\chi_\alpha)$ where the square of $\omega^{1/2}_{\chi_\alpha}$ is a numerical weight, $\chi_\alpha = \cos\theta_\alpha$ is a grid point in angle θ_α, and $P_{\mathbf{l}}$ is a Legendre polynomial. Then the potential $V(r, R, \theta)$ is approximated to be diagonal (unchanged) in this χ_α basis, but $\mathbf{j}^2$ and $\mathbf{l}^2$ are represented as $\mathbf{T}^+\mathbf{j}^2\mathbf{T}$ and $\mathbf{T}^+\mathbf{l}^2\mathbf{T}$, respectively, in this χ_α basis. The row dimension ($\mathbf{l}$) of the $\mathbf{T}$ matrix is equal to the number of basis functions when $\varphi^3_{\nu_3}(\theta)$ is expanded in terms of Legendre functions, and the column dimension (χ_α) of $\mathbf{T}$ is equal to the number of grid points when $\varphi^3_{\nu_3}(\theta)$ is expressed in a numerical grid representation. These two dimensions are the same in standard DVR calculations.

Equations 11a, 11b, and 11c are all transformed by the $\mathbf{T}$ matrix to give new equations that are defined at each grid point. In this representation, we calculate a numerical value of $\varphi^1_{\nu_1}(r)$, $\varphi^2_{\nu_2}(\mathrm{R})$, and $\varphi^3_{\nu_3}(\theta)$ at each grid point, say r_α, R_α, and θ_α, respectively. The finite difference method is then used to solve the differential equations numerically.

B. IOS Approximation. We turn to the determination of the final state wave function, $\Psi^{\mathrm{f}}_{\nu_1' j}(r, R, \theta)$, where ν_1' and j indicate vibrational and rotational quantum number of the product diatom AB, respectively. Here we assume that vibration may be separated from the other variables using

$$\Psi^{\mathrm{f}}_{\nu_1' j}(r, R, \theta) \approx \varphi^{\mathrm{d}}_{\nu_1'}(r)\, \psi^{\mathrm{E}}_j(R, \theta) \quad (13)$$

where $\varphi^{\mathrm{d}}_{\nu_1'}(r)$ is a vibrational wave function of the state ν_1' of diatom AB, which is a solution of the vibrational Schrödinger equation of diatom AB

$$\left[-\frac{1}{2\mu_1}\frac{\partial^2}{\partial r^2} + V_1(r)\right]\varphi^{\mathrm{d}}_{\nu_1'}(r) = E^{\mathrm{d}}_{\nu_1'}\varphi^{\mathrm{d}}_{\nu_1'}(r) \quad (14)$$

The continuum wave function $\psi^{\mathrm{E}}_j(R, \theta)$ consists of two parts—one is the rotational (j) motion of the diatom and the other is the relative translational motion of the diatom with respect to atom C. The Schrödinger equation for $\psi^{\mathrm{E}}_j(R, \theta)$ is

$$\left[-\frac{1}{2\mu_2}\frac{\partial^2}{\partial R^2} + \frac{1}{2\mu_2 R^2}\mathbf{l}^2 + \left\langle \varphi^{\mathrm{d}}_{\nu_1'}(r)\left|\frac{1}{2\mu_1 r^2}\right|\varphi^{\mathrm{d}}_{\nu_1'}(r)\right\rangle \mathbf{j}^2 + \langle \varphi^{\mathrm{d}}_{\nu_1'}(r)|V_2(r, R, \theta)|\varphi^{\mathrm{d}}_{\nu_1'}(r)\rangle - (E^{\mathrm{i}}_{\nu_1\nu_2\nu_3} - E^{\mathrm{d}}_{\nu_1'})\right]\psi^{\mathrm{E}}_j(R, \theta) = 0 \quad (15)$$

When the rotational motion is much slower than the translational motion during the dissociation, we can reasonably utilize the infinite order sudden (IOS) approximation. Under IOS, we set $\mathbf{j}^2 = \bar{j}(\bar{j}+1) = \mathbf{l}^2$, where the latter equality arises because total angular momentum is fixed as zero. Then the scattering equation we obtain is one-dimensional, i.e.

$$\left[-\frac{1}{2\mu_2}\frac{\partial^2}{\partial R^2} + \frac{1}{2\mu_2 R^2}\bar{j}(\bar{j}+1) + B\bar{j}(\bar{j}+1) + \bar{V}_2(R; \theta) - E\right]\varphi^{\mathrm{E}}_j(R; \theta) = 0 \quad (16)$$

Here B is the rotational constant of the diatom for vibrational state ν_1' (the third term in eq 15), $\bar{V}_2(R; \theta)$ is the averaged V_2 integral over $\varphi^{\mathrm{d}}_{\nu_1'}(r)$ (the fourth term in eq 15), E is the energy which is $E^{\mathrm{i}}_{\nu_1\nu_2\nu_3} - E^{\mathrm{d}}_{\nu_1'}$, and $\varphi^{\mathrm{E}}_j(R; \theta)$ parametrically depends on the angle θ. $\psi^{\mathrm{E}}_j(R, \theta)$ is here approximated as

$$\psi^{\mathrm{E}}_j(R, \theta) \approx \sqrt{(2j+1)/2}\,\varphi^{\mathrm{E}}_j(R; \theta)\, P_j(\theta) \quad (17)$$

where $P_j(\theta)$ is a Legendre function. In the present study we chose $\bar{j} = j$, where j is the final rotational quantum number.

Equation 16 is solved at various angles, θ, using a fifth-order Adams−Moulton algorithm with numerical grid representations of the wave functions. The number of angles chosen is equal to the number of grids used in solving eq 10c. The derived asymptotic form of $\varphi^{\mathrm{E}}_j(R; \theta)$ is

$$\varphi^{\mathrm{E}}_j(R;\theta) \to k^{-1}[\mathrm{e}^{-i(kR-(\bar{j}/2)\pi)} - \mathrm{e}^{i(kR-(\bar{j}/2)\pi)}\mathrm{e}^{2i\delta}] \quad (18)$$

where δ is a phase shift and k is a wave vector, i.e., momentum $p = \hbar k$. Since we calculate a real solution $\varphi^{\mathrm{E}}_{j,\mathrm{real}}(R; \theta)$ of eq 16, we need a conversion factor Q, where $\varphi^{\mathrm{E}}_j(R; \theta) = \varphi^{\mathrm{E}}_{j,\mathrm{real}}(R; \theta)Q$, to give the right boundary conditions. The real wave function we calculate has the asymptotic form

$$\varphi^{\mathrm{E}}_{j,\mathrm{real}}(R; \theta) \to k^{-1}\left[A(\theta)\sin\left(kR - \frac{\bar{j}}{2}\pi\right) + B(\theta)\cos\left(kR - \frac{\bar{j}}{2}\pi\right)\right] \quad (19)$$

where $A(\theta)$ and $B(\theta)$ are determined by evaluating eq 19 and its derivative at the asymptotic limit of R. After matching eq 19 to eq 18, we obtain the conversion factor Q and, at a given R and θ

$$\varphi^{\mathrm{E}}_j(R; \theta) = 2[B(\theta) + iA(\theta)]^{-1}\varphi^{\mathrm{E}}_{j,\mathrm{real}}(R; \theta) \quad (20)$$

The final state wave function $\psi^{\mathrm{f}}_{\nu_1' j}(r, R, \theta)$ therefore obtained from eqs 13, 17, and 20 is

$$\psi^{f}_{\nu_1' j}(r, R, \theta) = \varphi^{d}_{\nu_1'}(r)[B(\theta) + iA(\theta)]^{-1}\varphi^{E}_{j,\mathrm{real}}(R; \theta)\sqrt{(2j+1)/2}P_j(\theta) \quad (21)$$

C. Lifetime from DWBA. Now we want to compute the lifetime of the vibrationally excited triatomic van der Waals complex, which eventually dissociates into atom and diatom fragments. The dissociation process is assumed to be due to mode−mode correlation that causes energy transfer (and predissociation) from vibrational motion of the triatom. The correlation potential, V_c, is given by

$$V_c = H - H^{SCF} = \frac{1}{2\mu_1 r^2}\mathbf{j}^2 - \left\langle\frac{1}{2\mu_1 r^2}\right\rangle_r \mathbf{j}^2 - \frac{1}{2\mu_1 r^2}\langle\mathbf{j}^2\rangle_\theta + \frac{1}{2\mu_2 R^2}\mathbf{l}^2 - \left\langle\frac{1}{2\mu_2 R^2}\right\rangle_R \mathbf{l}^2 - \frac{1}{2\mu_2 R^2}\langle\mathbf{l}^2\rangle_\theta + V_2(r, R, \theta) - \langle V_2(r, R, \theta)\rangle_{R,\theta} - \langle V_2(r, R, \theta)\rangle_{r,\theta} - \langle V_2(r, R, \theta)\rangle_{r,R} - E_{\mathrm{cor}} \quad (22)$$

Note that our final wave function is three-dimensional and eq 18 is normalized to a unit incoming flux. Then the density of the final states at energy E, $\rho(E)$, is

$$\rho(E) = \frac{\mu_2 p}{(2\pi\hbar)^3} \quad (23)$$

Then the DWBA form of the predissociation rate R from the $(\nu_1\nu_2\nu_3)$ initial triatomic state to the $(\nu_1' j)$ final diatomic state given in eq 6), using eqs 7 and 10, can be rewritten as[20]

$$R(\nu_1\nu_2\nu_3 \rightarrow \nu_1' j) = \frac{2j+1}{2\pi^2\hbar^2 v}|\langle[B(\theta) + iA(\theta)]^{-1}P_j(\theta) \times \varphi^{E,N}_{j,\mathrm{real}}(R; \theta)\,\varphi^{d}_{\nu_1'}(r)|V_c(r, R, \theta)|\varphi^{1}_{\nu_1}(r)\,\varphi^{2}_{\nu_2}(R)\,\varphi^{3}_{\nu_3}(\theta)\rangle|^2 \quad (24)$$

or numerically

$$R(\nu_1\nu_2\nu_3 \rightarrow \nu_1' j) = \frac{2j+1}{2\pi^2\hbar^2 v}|\sum_{\theta_\alpha}\omega_{\theta_\alpha}[B(\theta_\alpha) + iA(\theta_\alpha)]^{-1}\Pi_j(\theta_\alpha)\,\varphi^{3}_{\nu_3}(\theta_\alpha) \times \sum_{R_\alpha}\omega_{R_\alpha}\varphi^{E,N}_{j,\mathrm{real}}(R_\alpha; \theta_\alpha)\varphi^{2}_{\nu_2}(R_\alpha)\sum_{r_\alpha}\omega_{r_\alpha}\varphi^{d}_{\nu_1'}(r_\alpha)\,\varphi^{1}_{\nu_1}(r_\alpha)\,V_c(r_\alpha, R_\alpha, \theta_\alpha)|^2 \quad (25)$$

where v is an asymptotic velocity and $\varphi^{E}_{j,\mathrm{real}}(R; \theta) = k^{-1}\varphi^{E,N}_{j,\mathrm{real}}(r; \theta)$. The half-width, Γ, is

$$\Gamma(\nu_1\nu_2\nu_3 \rightarrow \nu_1'_j) = \hbar R(\nu_1\nu_2\nu_3 \rightarrow \nu_1' j)/2 \quad (26a)$$

$$\Gamma(\nu_1\nu_2\nu_3 \rightarrow \nu_1') = \sum_j \Gamma(\nu_1\nu_2\nu_3 \rightarrow \nu_1' j) \quad (26b)$$

and the predissociation lifetime of the $(\nu_1\nu_2\nu_3)$ state of AB−C, τ is

$$\tau(\nu_1\nu_2\nu_3) = \frac{\hbar}{2\Gamma(\nu_1\nu_2\nu_3 \rightarrow \nu_1')} \quad (27)$$

III. Computational Details

We have utilized atom−atom pairwise Morse type potential energy functions, where the whole potential is assumed to be a sum of diatomic potentials, i.e., A−B, A−C, and B−C. The relevant Morse parameters, D_e (dissociation energy), β (exponential factor), and r_e (equilibrium distance) are listed in Table 1. For the He−ICl complex, we tested two kinds of Morse potential parameters. One is the atom−atom Morse potential parameters used by Gray et al.[13] (we call this the A type potential). The other is the potential parameters used by Waterland et al.[15] (B type potential). For He−I_2, Gray's potential parameters are used.[19] The electronic state of I_2 is the excited B state in which the I_2 has symmetry $^3\Pi_0^+$. We studied the $\nu = 2-5$ states of He−ICl and the $\nu = 12-26$ states of He−I_2. The electronic state of ICl is the excited B state. The atomic masses of He, Cl, and I are 7291, 63 746, and 231 332 au, respectively. In numerical integrations of the VSCF equations, the starting point, the end point, and grid size are repeatedly tested so that the optimum number of points are determined. For the internuclear distance of AB, i.e., the r-axis, integration is performed from 4.5 to 9.0 au with a grid of 0.002 au for He−ICl, and from 4.8 to 13.0 au with a grid of 0.002 au for He−I_2, respectively. Integration for the R-axis is from 4.5 to 30.0 au with a grid of 0.02 au for He−ICl, and from 6.0 to 30.0 au with a grid of 0.05 au for He−I_2, respectively. For all complexes, Legendre functions with $l = 0$ to 40 are used for θ axis basis functions. This corresponds to 41 grid points in the DVR scheme. What we have investigated are the vibrational energy levels $(\nu_1\nu_2\nu_3)$ of the bound AB−C complex, the dissociation rates from AB−C $(\nu_1\nu_2\nu_3)$ to AB$(\nu_1' = \nu_1 - 1, j)$ + C, the rotational distribution of AB(ν_1', j), and, consequently, lifetimes of AB−C (ν_1, ν_2, ν_3). We have assumed the strong propensity rule $\Delta v_1 = -1$, so that all $\Delta v_1 > -1$ transitions are neglected.

TABLE 1: Pairwise Morse Potential Function Parameters

complex	atom pair	D_e/cm^{-1}	β/au^{-1}	r_e/au
He−ICl				
A type	I−Cl	1270.4	2.0955	5.02667
	He−I[a]	18	0.6033	7.559
	He−Cl[a]	14	0.8467	6.8030
B type	I−Cl	1270.4	2.0955	5.02667
	He−I[b]	16.5	0.79377	7.5589
	He−Cl[b]	16.0	0.79377	7.5589
He−I_2	I−I	4600.19	0.9583	5.6955
	He−I[c]	15.4	0.695	7.5589

[a] Reference 13. [b] Reference 15. [c] Reference 19.

IV. Results and Discussion

The VSCF calculated vibrational energy levels of He−ICl and He−I_2 are presented in Tables 2 and 3 and compared with earlier theoretical results based on the same potentials (A type with ref 13 and B type with ref 15) and with experiment. The vibrational energy levels of ICl and I_2 are also listed to clearly show the dissociation energy of the process, e.g., He−ICl $(\nu_1 = 2, 0, 0) \rightarrow$ He + ICl $(\nu_1' = 1, j)$. We see that the (2, 0, 0) energies are in good agreement with previous theoretical results in both tables. This shows that the VSCF method is useful for determining vibrational energy levels for van der Waals complexes. However, the excited bend states in Table 2 are not as close. Fortunately, these excited states are not the primary concern of this study, as the only experimental results are for ground-state bends.

The vibrational energy levels of diatomic ICl and I_2 are exactly calculated, so we do not include comparisons with other results. The predissociation process of interest in this work is AB − C$(\nu_1, \nu_2, \nu_3) \rightarrow$ AB$(\nu_1 - 1, j)$ + C. Therefore for this process the total energy for dissociation is the vibrational energy

TABLE 2: VSCF Vibrational Energy Levels (cm^{-1}) of He−ICl and ICl

	this work				others	
(ν_1, ν_2, ν_3)	A type		B type		theoretical	exptl
			HeICl			
(0, 0, 0)		(−13.9734)[a]		(−12.7130)[a]		
(2, 0, 0)	384.9063	(−13.9212)	384.9278	(−12.6393)	−13.331[b]	
(2, 0, 1)	389.8243	(−9.0033)	391.0189	(−6.5482)	−7.738[b]	
(2, 0, 2)	391.8766	(−6.9509)	393.2348	(−4.3324)	−6.294[b]	
(2, 0, 3)	394.6519	(−4.1756)	396.1263	(−1.4408)	−5.215[b]	
(2, 0, 4)	398.1617	(−0.6658)		not bound	−3.725[b]	
(2, 0, 5)		not bound		not bound	−1.504[b]	
(3, 0, 0)	548.4346	(−13.8903)	548.4654	(−12.5991)	−14.6[c]	−15[d]
(5, 0, 0)	817.6534	(−13.8140)	817.7086	(−12.4985)		
			ICl			
ν_1	E_{ν_1}		ν_1	E_{ν_1}		
0	e		3	548.3515		
2	384.8541		5	817.4940		

[a] The numbers in parentheses are the energy difference between He−ICl(ν_1, ν_2, ν_3) and ICl(ν_1). [b] Reference 15. The energy is the difference between He−ICl(ν_1, ν_2, ν_3) and ICl(ν_1). [c] Reference 13. The energy is the difference between He−ICl(ν_1, ν_2, ν_3) and IC l(ν1). [d] Reference 36.[e] The ground vibrational energy is -1162.1418 cm^{-1} with respect to the I + Cl separate atom limit.

TABLE 3: VSCF Vibrational Energy Levels (cm^{-1}) of He−I_2 and I_2

		He−I_2		
(ν_1, ν_2, ν_3)	$E^{SCF}_{\nu_1\nu_2\nu_3}$		(ν_1, ν_2, ν_3)	$E^{SCF}_{\nu_1\nu_2\nu_3}$
(0, 0, 0)		(−13.8377)[a]	(20, 0, 0)	2152.8359
		(−13.8381)[b]	(20, 0, 1)	2159.1886
		(−13.7481)[c]	(20, 0, 2)	2162.7280
		(−13.4)[d]	(20, 0, 3)	2163.6930
(12, 0, 0)	1369.7972		(20, 1, 0)	2165.6360
(14, 0, 0)	1576.0096		(21, 0, 0)	2242.8762
(16, 0, 0)	1775.2544		(22, 0, 0)	2331.1743
(17, 0, 0)	1872.2624		(25, 0, 0)	2585.6169
(18, 0, 0)	1967.5289		(26, 0, 0)	2666.9471
(19, 0, 0)	2061.0533			
		I_2		
ν_1	E_{ν_1}		ν_1	E_{ν_1}
0	*e*		19	2074.6201
12	1383.4766		20	2166.3848
14	1589.6590		21	2256.4069
16	1788.8711		22	2344.6865
17	1885.8633		25	2599.0607
18	1981.1130		26	2680.3803

[a] VSCF value (this work). This energy is the difference between He−I_2(0, 0, 0) and I_2(0). [b] VSCF value (reference 27). [c] CI value (reference 27). [d] CI value (reference 26). [e] The ground vibrational state energy is −4537.1084 cm^{-1} with respect to the I + I separated atom limit.

TABLE 4: Predissociation Lifetimes (ns) for He−ICl (ν_1, 0, 0) → He + ICl (ν_1 − 1)

	this work			
ν_1	A type	B type	theoretical	exptl
2	2.37	1.42	2.18[a]	<2.0[b]
3	1.23	0.72	1.00[c]	0.55[d]
5	0.51	0.24		

[a] Reference 15. [b] Reference 10. [c] Reference 16. [d] Reference 13.

difference between AB−C(ν_1, ν_2, ν_3) and AB(ν_1 − 1). A portion of the total energy is consumed to break the van der Waals AB−C bond, and the remaining energy is, after dissociation, distributed to the rotational energy of AB and relative kinetic energy of AB against C.

Table 4 presents the predissociation lifetimes of He−ICl (ν_1(=2, 3, or 5), 0, 0), where the only dissociation process considered is He−ICl(ν_1, 0, 0) → He + ICl(ν_1 − 1, *j*). When the vibrational quantum number of ICl is smaller by 2 or more than the corresponding ν_1 of He−ICl, the predissociation rate is very small. As expected, the lifetime of He−ICl (ν_1 = 2, 0, 0) is longest and that of ν_1 = 5 is shortest. This is due to the fact that the energy difference between He−ICl (ν_1, 0, 0) and ICl (ν_1 − 1, *j*) is largest when ν_1 = 2 and smallest when ν_1 = 5. Depending on the potential used (A or B type), the calculated lifetimes vary 2-fold. The measured lifetime of He−ICl (2, 0, 0) is in the range of 0.5−2.0 ns.[10] Our value is 2.37 ns for the A type potential and 1.42 ns for B type, while Waterland et al.'s theoretical value is 2.18 ns.[15] These theoretical values are in reasonable agreement with each other. Waterland et al.'s calculations are more accurate than ours, but their method is far more complex.

The rotational state distributions of the fragment ICl from He−ICl are presented in Figures1 and 2. Note that we show B type results in Figure 1 and A type in Figure 2, so as to make comparisons with other theory for the same potential. For the He−ICl(2, 0, 0) → He + ICl(1, *j*′), the rotational distribution of ICl oscillates with the rotational quantum number *j* of ICl when *j* is less than 10. At *j* = 7, a prominent peak is noted. At large *j*'s, another broad peak is found around *j* = 15. This feature of the distribution is also found in experiments.[16] The rotational distribution profile of Waterland et al.'s[15] theoretical work is very similar to ours in Figure 1, but the magnitude of

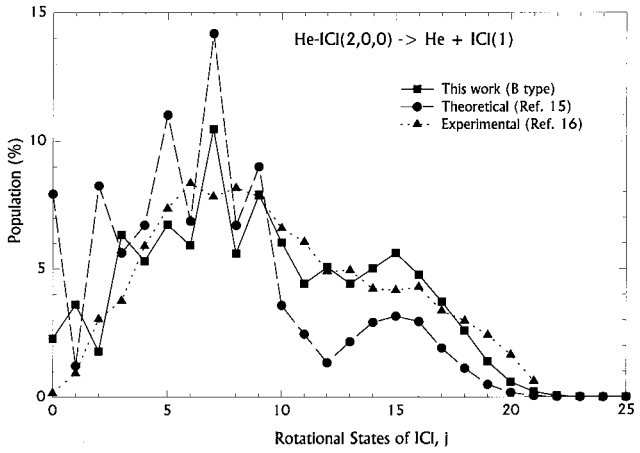

Figure 1. Rotational distribution of ICl(1, *j*) fragment from predissociation of He−ICl (2, 0, 0).

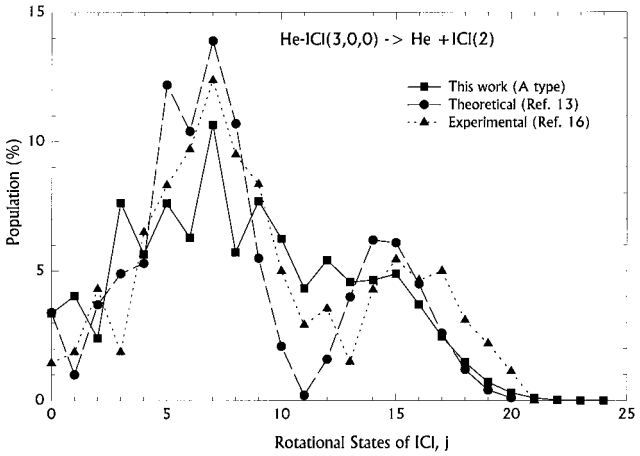

Figure 2. Rotational distribution of ICl(2, *j*) fragment from predissociation of He−ICl (3, 0, 0).

their oscillations is somewhat larger than ours. Averaging the oscillation at small *j*, this distribution process looks bimodal. As seen in Figure 2, the dissociation process of He−ICl(3, 0, 0) → He + ICl(2, *j*) is also bimodal. The theoretical results in Figure 2 are from Gray and Wozny[13] and show oscillations that are similar to what we find.

Though there are still discrepancies between our theoretical distributions and those of other theories in Figures 1 and 2, the overall trends are similar. This shows that the approximations we have made (SCF, DWBA, IOS) are not too serious for He−ICl. Differences between theory and experiment are probably due to inaccuracy of the potential functions used in the theoretical calculations.

Since the predissociation rates for the various excited states of He−I_2 have been reported,[17,19,33] we have investigated the predissociation dynamics of many excited states of the He−I_2 complex. The levels of He−I_2(ν_1, 0, 0) studied are from $\nu_1 = 12$ to $\nu_1 = 26$. Using the strong propensity rule for $\nu_1(HeI_2) \rightarrow (\nu_1 - 1)(I_2)$, we neglect lifetime contributions from other choices of $\Delta\nu_1$. The vibrational predissociation rates and corresponding lifetimes of the bound state of the He−I_2 complex are compiled in Table 5. The lifetime of the lower vibrational states (ν_1) of He−I_2 is longer than the higher ones. From the comparison with experimental measurements,[33] we see that our theoretical rates or lifetimes are in good agreement (10%) with experiment. The predissociation rates are plotted against initial vibrational levels in Figure 3. The calculated rates are lower than the experimental ones for high vibrational states.

TABLE 5: Total Vibrational Predissociation Rates and Lifetimes for He−I_2

	rate/10^9 s^{-1}		lifetime/ps	
ν_1	this work	exptl[a]	this work	exptl[a]
12	5.5		183	
14	6.7		150	
16	8.0		125	
17	8.7	7.8 ± 0.2	115	128 ± 2
18	9.4	8.7 ± 0.7	106	115 ± 9
19	10.2	9.9 ± 0.4	98	101 ± 4
20	11.0	10.6 ± 0.5	91	94 ± 4
21	11.9	12.2 ± 0.6	84	82 ± 4
22	12.6	13.3 ± 1.0	79	75 ± 6
23	13.7	15.6 ± 1.2	73	65 ± 5
24	14.5		69	
25	15.6		64	
26	16.7		60	

[a] Reference 33.

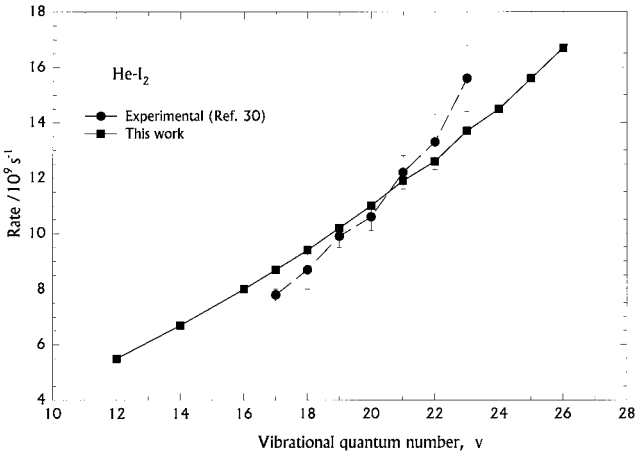

Figure 3. Vibrational predissociation rates of He−I_2(ν, 0, 0).

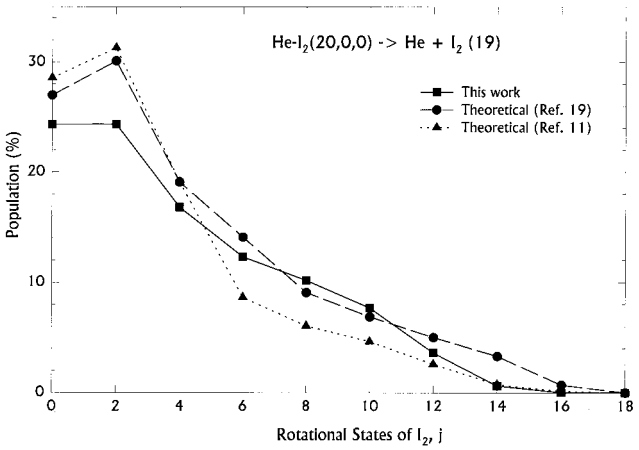

Figure 4. Rotational distribution of I_2(19, *j*) fragment from predissociation of He−I_2 (20, 0, 0).

The rotational distribution of the fragment I_2 is presented in Figures 4, 5, and 6. There is no particular reason why only the three states, i.e., $\nu_1 = 20$, 25, and 26, are presented. They are simply some examples for presentation. Since I_2 is a homonuclear diatomic molecule, the distribution cannot generally be bimodal. Unfortunately experimental measurements of the distribution have not been reported, to our knowledge. But comparisons with other various theoretical calculations[11,17,19] indicate that our distributions are reasonable.

The main purpose of this work is to test a simple theoretical tool for investigating the vibrational predissociation process of

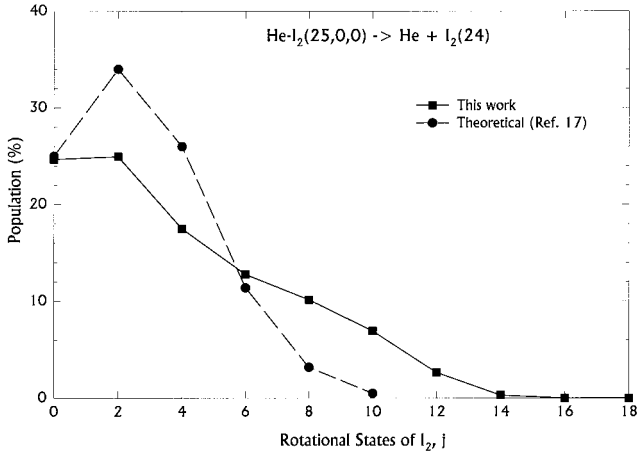

Figure 5. Rotational distribution of $I_2(24, j)$ fragment from predissociation of He−I_2 (25, 0, 0).

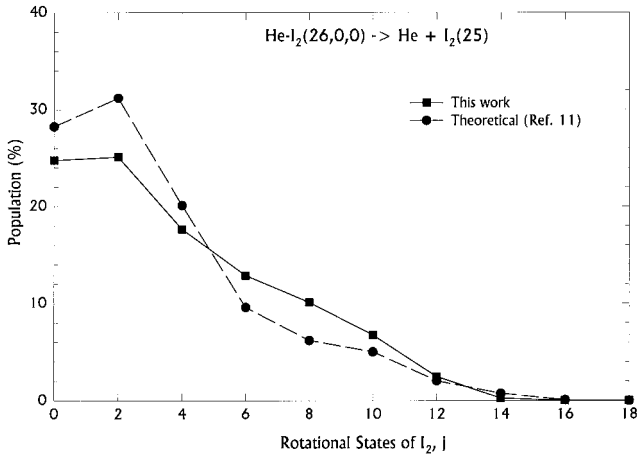

Figure 6. Rotational distribution of $I_2(25, j)$ fragment from predissociation of He−I_2 (26, 0, 0).

van der Waals complexes having a weak bond. The VSCF approximation used to locate the resonance energies of vibrationally excited van der Waals complexes is found to be accurate enough as shown in Table 2. We have not investigated dissociation of the bending excited vibrational states of the complexes. This will be studied in the near future. The distorted wave Born approximation is found to be valid at least for the systems we studied. Our calculated rates or lifetimes are in good agreement with experiments[33] as shown in Table 5. As presented in Figures 1, 2, and 4−6, the rotational state distributions of the diatomic fragments are also investigated to test the validity of IOS more stringently. IOS is found to be in reasonable agreement with other theoretical or experimental results, suggesting that the IOS approximation is reasonable. However one should be cautious that the IOS approximation may be valid for systems like He−ICl or He−I_2 but may not be so for other systems.

V. Conclusion

In this article we have presented a new and simple method for calculating the rates of vibrational predissociation in triatomic van der Waals complexes. This VSCF−DWBA−IOS method combines together three well-known approximations: the self-consistent field method for calculating the vibrational energy levels and wave functions of the initial metastable state, the infinite order sudden approximation for treating diatomic rotation in the final continuum state, and the distorted wave approximation for calculating the dissociation rates. Since the VSCF corresponds to an effective averaged potential, the correlation potential of eq 22 is the only one causing temporal evolution of the VSCF states. Therefore we might expect its approximate treatment, using DWBA, to be quite accurate (for similar reasons that Möller−Plesset perturbation theory is useful to improve VSCF energetics).[34,35]

We have presented applications of this theory to vibrational predissociation in the He−ICl and He−I_2 complexes. Both dissociation rates and product state distributions have been compared to the results from other theory (typically from accurate coupled channel or wave packet calculations) and from experiment. The agreement with both is generally quite good, which indicates that the combination of these three approximations is effective in describing these systems.

Calculations of vibrational predissociation rates for triatomic clusters, though not computationally trivial, are certainly feasible today by numerically exact quantum-mechanical algorithms. The usefulness of the present method lies, however, in the fact that it can be extended to much larger systems, while retaining its computational simplicity. For such larger systems, exact quantum calculations are not feasible at present. Consider, for example, the predissociation process: $M-AB(v) \rightarrow M + AB(v-1)$, where AB is a diatomic chromophore and M is a polyatomic molecule or a cluster to which AB is weakly bound. An extension of our method to this process seems straightforward. There are some complications not present in the case where M is an atom; for example, the final states of M will have to be described by VSCF if M is a polyatomic. This leads to a DWBA rate expression that involves multidimensional integrals. However, it seems that the required computational effort should be manageable for M having at least several atoms. The present study is therefore an encouraging test, showing that computational treatment of vibrational predissociation based on VSCF, IOS, and DWBA and thus application to larger systems seem desirable.

Acknowledgment. H.S. thanks Dr. Carl Williams for helpful discussions, and MOST/STEPI and Ministry of Education, Korea (BSRI-97-3409), for financial support. J.S. acknowledges the Korea Research Foundation for financial support. G.C.S. acknowledges NSF Grant CHE-9527677, and M.A.R. acknowledges NSF Grant CHE-9414699.

References and Notes

(1) Janda, K. *Adv. Chem. Phys.* **1985,** *60*, 201. Lester, M. I. *Adv. Chem. Phys.* **1996**, *96*, 51. Janda, K. C.; Roncero, O.; Halberstadt, N. *J. Chem. Phys.* **1996**, *105*, 5830.

(2) Miller, R. E. *J. Phys. Chem.* **1986**, *90*, 3301.

(3) Hutson, J. M. *Annu. Rev. Phys. Chem.* **1990**, *41*, 123.

(4) Le Roy, R. J.; Carley, J. S. *Adv. Chem. Phys.* **1980**, *42*, 353.

(5) Levy, D. H. *Adv. Chem. Phys.* **1981**, *47*, 323. Smalley, R. E., Wharton, L.; Levy, D. H. *J. Chem. Phys.* **1978**, *68*, 671.

(6) Nejad-Sattari, M.; Stephenson, T. A. *J. Chem. Phys.* **1997**, *106*, 5454. Roncero, O.; Halberstadt, N.; Beswick, J. A. *J. Chem. Phys.* **1996**, *104*, 7554.

(7) Beswick, J. A.; Jortner, J. *J. Chem. Phys.***1978**, *68*, 2277.

(8) Gerber, R. B.; McCoy, A. B.; Garcia-Vela, A. *Annu. Rev. Phys. Chem.* **1994**, *45*, 275.

(9) Balint-Kurti, G. G.; Shapiro, M. *Adv. Chem. Phys.* **1985**, *60*, 403.

(10) Lipkin, N.; Moiseyev, N.; Leforestier, C. *J. Chem. Phys.* **1993**, *98*, 1888.

(11) Zhang, D. H.; Zhang, J. Z. *J. Phys. Chem.* **1992**, *96*, 1575.

(12) Fang, J. -Y.; Guo, H. *J. Chem. Phys.* **1995**, *102*, 1944.

(13) Gray, S. K.; Wozny, C. E. *J. Chem. Phys.* **1991**, *94*, 2817.

(14) Manolopolous, D. E.; Stark, K.; Werner, H. -J.; Arnold, D. W.; Bradforth, S. E.; Neumark, D. M. *Science* **1993**, *260*, 1605.

(15) Waterland, R. L.; Lester, M. I.; Halberstadt, N. *J. Chem. Phys.* **1990**, *92*, 4261.

(16) Waterland, R. L.; Skene, J. M.; Lester, M. I. *J. Chem. Phys*. **1988**, *89*, 7277.

(17) Beswick, J. A.; Delgado-Barrio, G. *J. Chem. Phys.* **1980**, *78*, 3653.

(18) Neuhauser, D.; Judson, R. S.; Koury, D. J.; Adelman, D. E.; Shafer, N. E.; Kliner, D. A. V.; Zare, R. N. *Science* **1992**, *257* , 519.

(19) Gray, S. K. *Faraday Discuss*. **1994**, *97*, 143. Roncero, O.; Gray, S. K. *J. Chem. Phys*. **1996**, *104*, 4999.

(20) Schatz, G. C.; Gerber, R. B.; Ratner, M. A. *J. Chem. Phys*. **1988**, *88*, 3709.

(21) Bacic, Z.; Light, J. C. *Annu. Rev. Phys. Chem*. **1989**, *40*, 469.

(22) Bowman, J. M. *Acc. Chem. Res*. **1986**, *19*, 202. Jelski, D.; Haley, R. H.; Bowman, J. M. *J. Comput. Chem*. **1996**, *17*, 1645.

(23) Gerber, R. B.; Ratner, M. A. *J. Phys. Chem*. **1988**, *92* , 3252. Ratner, M. A.; Gerber, R. B. *J. Phys. Chem*. **1986**, *90*, 20.

(24) Thompson, T. C.; Truhlar, D. G. *Chem. Phys. Lett*. **1980**, *75*, 87.

(25) Clary, D. C.; Knowles, P. J. *J. Chem. Phys*. **1998**, *93*, 6334. Xie, D.; Yan, G. *Int. J. Quantum Chem*. **1998**, *66*, 119.

(26) Horn, T. R.; Gerber, R. B.; Ratner, M. A. *J. Chem. Phys*. **1989**, *91*, 1913.

(27) Seong, J.; Sun, H. *Bull. Korean Chem. Soc*. **1996**, *17*, 934.

(28) Gerber, R. B. *Chem. Phys*. **1976**, *21*, 1.

(29) Eno, L.; Balint-Kurti, G. G. *J. Chem. Phys*. **1979**, *71*, 1447.

(30) Levine, R. D. *Quantum Mechanics of Molecular Rate Processes*; Clarendon Press: Oxford, 1969.

(31) Bacic, Z.; Light, J. C. *J. Chem. Phys*. **1986**, *85*, 4594.

(32) Light, J. C.; Hamilton, I. P.; Lill, J. V. *J. Chem. Phys*. **1985**, *82*, 1400.

(33) Gutmann,M.; Willberg, D. M.; Zewail, A. H. *J. Chem. Phys*. **1992**, *97*, 8037.

(34) Hehre, W.; Radom, L.; Schleyer, P. R.; Pople, J. A. *Ab-Initio Molecular Orbital Theory*; Wiley: New York, 1986.

(35) Norris, L. S.; Ratner, M. A.; Roitberg, A. E.; Gerber, R. B. *J. Chem. Phys*. **1996**, *105*, 11261.

(36) Skene, J. M.; Drobits, J. C.; Lester, M. I. *J. Chem. Phys*. **1986**, *85*, 2329.